Design and performance of a 40W uplink laser transmitter for NASA's O2O laser communications mission

Katia Shtyrkova*[a], Clement D. Burton[a], Robert T. Schulein[b], Igor Gaschits[a], Barry Romkey[a], David O. Caplan[a], Daniel V. Murphy[a], Bryan S. Robinson[a]
[a]MIT Lincoln Laboratory, Lexington, MA USA;
[b]Bay Engineering Innovations, MD, USA.

ABSTRACT

NASA's Orion Artemis II Optical Communications System (O2O) will provide operational laser communications between the ground and lunar orbit for the Artemis II crewed mission. In this work we describe a 40 W ground-based laser transmitter for the O2O system. The uplink transmitter operates in the optical C-band and uses an energy-efficient 32-PPM modulation format. Four spatial diversity channels are time-aligned and combined in the far field. Each channel produces up to 10 W of output power and contains both the communications signal and the 7 kHz modulated beacon signal required for acquisition. The transmitter delivers data at 10 Mbits/s and 20 Mbits/s channel rates, corresponding to the 250 MHz and 500 MHz slot rates respectively.

Keywords: free-space optical communications, laser communications, lasercom, laser transmitter, O2O

1. INTRODUCTION

NASA's plan for future space exploration includes several consecutive missions each designed to further mature the technology necessary to return humans to the moon and beyond [1, 2]. As part of this path, Artemis I was a successful 25-day uncrewed lunar flyby mission launched in Nov. 2022 [3]. It demonstrated the successful operation of Orion spacecraft and Space Launch System (SLS) rocket. Artemis II is a follow-on crewed mission to be launched on the SLS rocket, where the Orion capsule will carry four astronauts around the Moon. The mission will use an S-band phased array antenna with data rates up to ~6 Mbps from lunar distances to send data to/from NASA's Deep Space Network (DSN) on the ground. To enhance available mission data rates, the Orion capsule will be equipped with a free-space laser communications terminal. O2O (Orion Artemis II Optical) communications system will provide up to 260 Mbps return links from space to ground and up to 20 Mbps forward link to the Orion module at lunar distances, far surpassing the capabilities of the S-band antenna [4, 5]. Table 1 lists all supported O2O mission data rates. Such data rates will provide additional mission capabilities, such as real-time video conferencing from lunar distances, real-time large volume file transfers, and the ability to downlink most of the mission data during the flight [5].

Table 1. Supported O2O mission data rates.

Link Direction	Data Rates (Mbps)
Up / Forward	10, 20*
Down / Return	20, 40, 80*, 130, 190, 260

A high-level O2O architecture is as follows: the mission is directed from the Mission Control Center (MCC) at Johnson Space Center (JSC) in Houston, TX. All Orion user data and commands originate and terminate either at Orion spacecraft or at the MCC. For the S-band RF comm link, the data flows from the MCC to DSN to Orion spacecraft, and back in the

*katia.shtyrkova@ll.mit.edu; www.ll.mit.edu

This material is based upon work supported by the National Aeronautics and Space Administration under Air Force Contract No. FA8702-15-D-0001. Any opinions, findings, conclusions or recommendations expressed in this material are those of the author(s) and do not necessarily reflect the views of the National Aeronautics and Space Administration.

reverse order. For optical communications, the data will flow from the MCC to the Ground Data Element (GDE) at NASA White Sands Complex (WSC) in New Mexico, USA, which serves as a central intermediary between the MCC and the two optical ground stations [6]. The GDE ultimately sends and received user data (in form of Ethernet packets) to and from the optical ground stations. The two primary optical ground stations for the O2O mission are located at NASA's WSC in New Mexico (managed by NASA) and at Table Mountain, California (managed by Jet Propulsion Laboratory [7]). It is expected that weather and atmospheric conditions would be deciding factors on which ground station is used at any particular time during the mission. The ground stations communicate to the space-based laser communications terminal onboard the Orion spacecraft [5], which has a 10cm aperture and transmits up to 1W of average optical power to the ground. This work focuses on the design and characterization of the uplink laser transmitter for WSC ground station, necessary to close the link with the Orion's space-based lasercom terminal at the pre-defined user data rates of 10 Mbps and 20 Mbps.

System requirements

Uplink transmitter requirements for the WSC optical ground station were derived from a detailed link budget designed to deliver a required amount of optical power to the spacecraft receiver at lunar distances and assuming that the uplink telescope previously used for the Lunar Laser Communications Demonstration (LLCD) mission [8, 9] would be reused for the O2O. This existing uplink telescope has four 15-cm individual refractor telescopes that form a single beam in the far field, making it a four-channel system [10]. Table 2 lists supported uplink communication modes, and Table 3 lists a subset of high-level requirements for the uplink transmitter that guided its design and implementation.

Table 2. Uplink Communication Modes

Slot Rate	Slot Width	Code Rate	Modulation Format	Data Rate
250 MHz	4 ns	1/3	PPM-32	~10 Mbps
500 MHz	2 ns	1/3	PPM-32	~20 Mbps

Table 3. High-level uplink transmitter requirements [11]

Waveform	
Communication modes:	Two uplink comm modes listed in Table 2
Pulse shape:	50% return-to-zero raised cosine
Inter-channel delay:	<50 ps
Extinction ratio:	≥25 dB
Signaling	
Signals/channel:	One acquisition and one comm beam per channel
Comm signals:	$\lambda_{UL\ COMM}$=154x.x nm, x 4 channels; spaced by $\Delta\lambda_{COMM\ MIN}$, bound by $\Delta\lambda_{COMM\ Bound}$
Acquisition signals:	λ_{BEACON}=153x.x nm, x 4 channels; spaced by $\Delta\lambda_{BEACON\ MIN}$, bound by $\Delta\lambda_{BEACON\ Bound}$ λ_{FILLER}=153x.x nm, x 4 channels; spaced by $\Delta\lambda_{FILLER\ MIN}$, bound by $\Delta\lambda_{FILLER\ Bound}$
Acquisition modulation:	~ 7 kHz square wave for λ_{BEACON}
Output Power	
Aggregate power:	40 W average, 10 W / channel x4 channels, shared between comm and acquisition Ability to step down the power in 3 dB steps
Comm/Acquisition power:	Adjust ratio of acquisition to comm signals at the output in 3 dB steps, in < 2s Provide acquisition-only beam at all required power levels
Other	
	Provide health and telemetry
	Meet all listed requirements with the length of output fiber out of the high-power optical amplifier <2.5m

2. DESIGN / IMPLEMENTATION

System Overview

High-level schematic of the uplink transmitter is shown in Figure 1. The transmitter consists of four low power optical channels that connect to high power optical amplifiers (HPOAs) via four single mode fibers which in turn connect to four uplink transmit telescopes, each with 15.4 cm aperture. HPOAs provide up to 10W of average output power each, for a total of 40W of combined output power out of the transmitter.

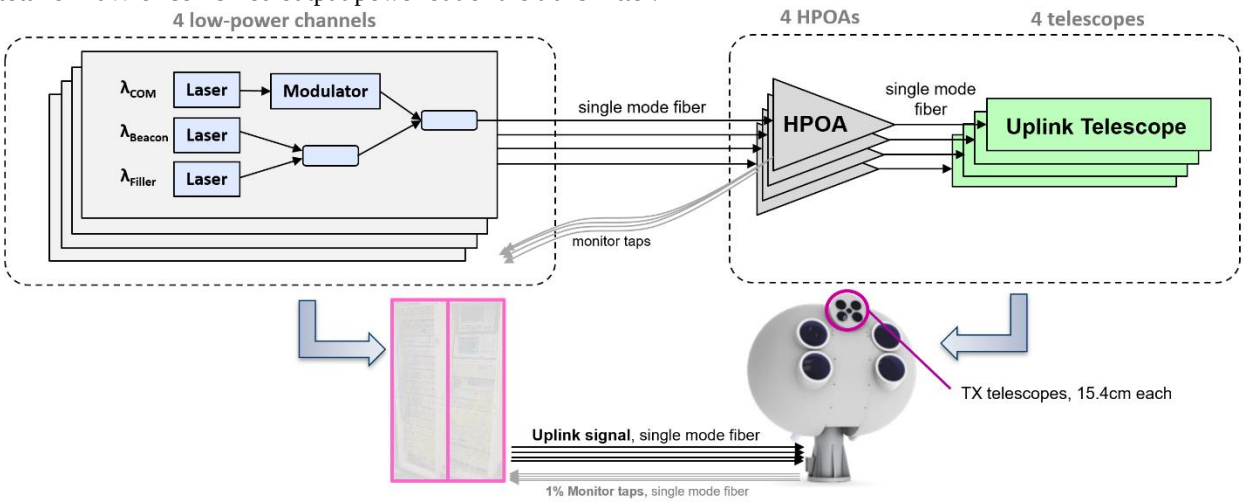

Figure 1. Uplink transmitter high-level schematic.

Each low power channel includes electro-optics to produce uplink communications waveform, as well as the acquisition signals (beacon / filler). The four low power channels carry identical user data / acquisition signals, are time-aligned at the output of the telescopes, and spatially overlap in the far field producing a single transmit beam for the spacecraft receiver. This four-channel architecture is done for several reasons, such as avoiding having a single 40W HPOA with corresponding nonlinearities to manage, improving spatial diversity which avoids the need for adaptive optics on the uplink beam, and cost reduction by leveraging the telescope system used for a previous program (LLCD, [10, 12]). Individual uplink comm wavelengths of the four channels are specified in [11]. There is a minimum separation between the four uplink comm wavelengths, necessary to avoid the receiver performance degradation due to coherent interference [13]. There is also a maximum wavelength separation, dictated by the bandwidth of the narrowband optical filter at the space terminal's receiver. There are similar limits on the acquisition wavelengths, though they do not pass through a narrowband optical filter. All system wavelengths are constantly monitored and adjusted to prevent drifting out of specification.

Physically, the system is composed of two 42U (1U = 1.75 inches) racks (see Figure 6) which are connected via single mode optical fibers to an enclosed gimballed mount which houses the telescopes. The two racks house all low power hardware, all diagnostic equipment, the main computer to control the system, as well as the hardware necessary to monitor transmitted signal. The gimballed mount houses uplink telescopes, pointing / acquisition and tracking (PAT) hardware, high-power optical amplifiers, and downlink/receive telescopes. The uplink transmitter is entirely fiber-based (i.e., no free-space components) until the high-power signals couple into the uplink telescopes.

Data formatter / Comm signal path

The high-level architecture of the data formatter and communications signal path is shown in Figure 2. User data in the form of asynchronous Ethernet frames is mapped into a Consultative Committee for Space Data Systems (CCSDS)-compatible [14] waveform of binary vectors with Serially Concatenated Pulse Position Modulation (SCPPM) encoding [15] and convolutional channel interleaving using an FPGA-based data formatter [16, 17]. Slot rate / effective data rate is selected from two implemented uplink modes (10 Mbps and 20 Mbps) listed in Table 2. Interleaver depth is user-selected from a set of pre-defined values based on the state of the atmospheric channel. In the absence of user data, the FPGA generates fill frames. The data formatter is also capable of producing any of the downlink modes (Table 1) for testing the receiver. Data formatter output goes into a 1x4 RF distribution box, which splits the signal onto the four identical RF channels that subsequently drive the four Mach-Zehnder modulators, one in each of the four parallel uplink transmitters.

Each RF channel has a voltage-controlled phase shifter ($\Delta\varphi_i$ in Figure 2) operating at either 500 MHz or 250 MHz clock rate, allowing the per-channel time-alignment.

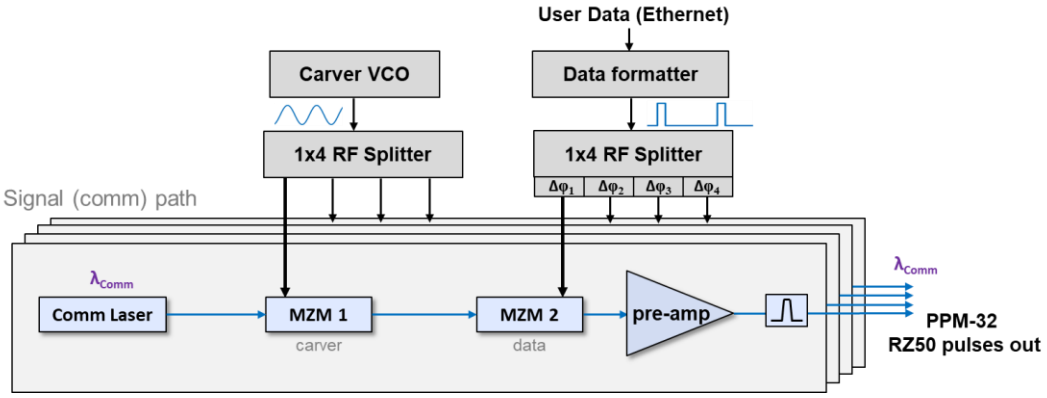

Figure 2. Data formatter / Comm signal path schematic.

Pulse-carved 50% return-to-zero (RZ50) data waveform generation is implemented by cascading two Mach-Zehnder modulators (MZMs), where the first MZM carves out RZ50 pulses from a CW source laser at a specified slot rate, while the second modulator encodes user data from the data formatter onto the pulses carved by the first MZM.

A voltage-controlled oscillator (VCO) is used to create a 250 MHz or 500 MHz sinusoidal RF signal ultimately used to drive the four carving MZMs. The output of the VCO goes through a 1x4 RF splitter and subsequent RF amplifiers to provide the driving voltages to MZMs in all four channels. In order to carve the RZ50 pulses, the carver MZMs are biased at quadrature and sinusoidally driven from transmission null to peak with an amplitude of V_π. While the phase of the VCO output signal is adjustable, there is no individual channel-based phase control. In each channel, the carver MZM is followed by a data MZM, as shown in Figure 2, which imparts the on and off pulse position modulation (PPM) data onto the waveform. "Data" optical pulses need to be time-aligned to carver-produced RZ50 pulses. This is accomplished by adjusting the per-channel phase of the RF signals driving data MZMs using voltage-controlled phase shifters in the 1x4 RF data pulse distribution box.

The electro-optic path for each comm signal channel starts with a continuous wave (CW) distributed feedback (DFB) laser at a specified wavelength, followed by the carver (MZM1) and data modulator (MZM2). The comm signal then passes through an optical pre-amplifier and a Fiber Bragg Grating (FBG) bandpass filter that removes the amplified spontaneous emission (ASE), prior to being combined with the acquisition signal wavelengths.

Acquisition signal path

A diverged beacon is used for spatial acquisition at the spacecraft. After initial acquisition, a narrow-beam beacon signal is used for tracking. Each acquisition path starts with two DFB lasers – one at a specified beacon wavelength, and another at a specified "filler" wavelength (Table 3, [11]), as shown in Figure 3. To meet the requirements of the spacecraft terminal acquisition sensor, the beacon signal needs to be square-wave-modulated at ~7 kHz. Such pulse width / duty cycle manifests in cross-gain modulation and other undesirable time-domain effects when injected into a high-power optical amplifier (HPOA). Therefore, an additional wavelength, termed "filler" is used to mitigate those effects is such a way that the acquisition signal essentially appears as a CW input to the HPOA as in [12, 13]. The beacon and filler lasers are combined via a fast optical switch driven by a 7 kHz square wave from a commercial frequency generator in such a way that every half a cycle either beacon or filler signal is present (shown in Figure 3[b]). The relative powers of beacon and filler signals are adjusted so that they are equal at the output of the HPOA and minimize distortions of the comm signal. The filler wavelength is filtered out by the spacecraft optical terminal, and therefore does not affect system comm performance.

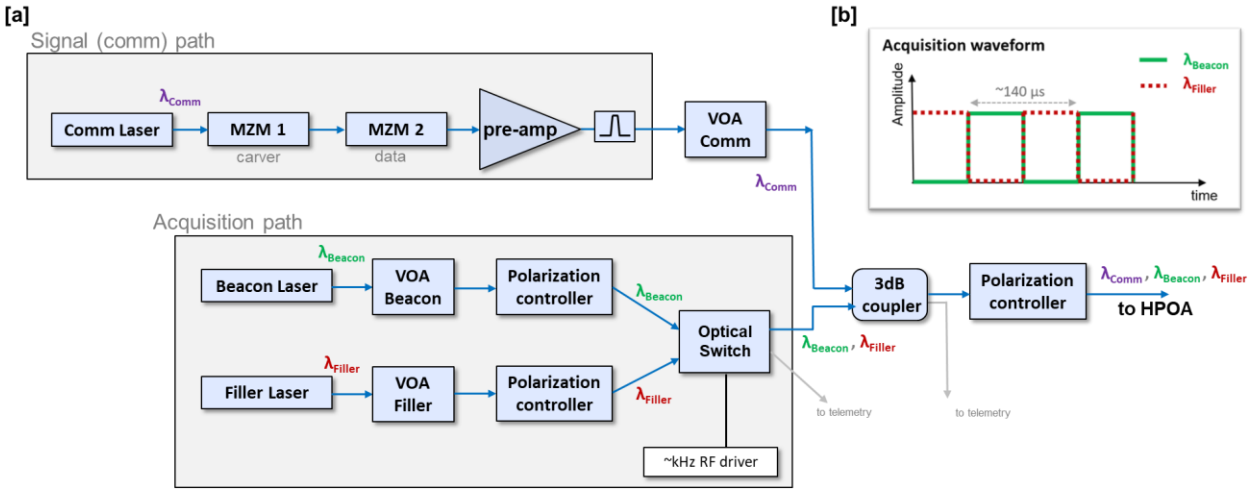

Figure 3. Uplink comm signal and acquisition signal electro-optics

As the system transitions from spatial acquisition (beacon-signal-dominated) to coarse and fine tracking and comm (uplink comm-signal-dominated), the amount of beacon and uplink comm signals at the output of HPOAs need to be adjusted rapidly as specified in Table 3. To enable this, variable optical attenuators (VOAs) are placed into beacon, filler and comm paths as shown in Figure 3, in a way that allows adjusting the power of each signal independently before they are coupled into the HPOA. HPOA gain is dependent on wavelength and specified output power. The three transmitter signals (comm, beacon and filler) experience different gain as they go through the amplifier at each of the specified output power settings, which is compensated for by adjusting the VOAs accordingly. The acquisition/comm ratio at the output of the transmitter is constantly monitored and adjusted as needed to meet the specified set points.

Comm signal and the beacon/filler signal are combined via a 3-dB fiber coupler, with one output being used for telemetry and another as the HPOA input. Voltage-controlled polarization controllers allow for independent control of beacon and filler polarizations separately, as well as the combined polarization of beacon/filler/comm signal. This provides the flexibility needed to mitigate polarization-dependent nonlinear effects after the HPOA, further described in the System Performance /Characterization section of this paper.

Time alignment

Each of the four low power channels is coupled into an individual HPOA with a single-mode (at optical C-band) fiber. Per system requirements, the four signals need to be time-aligned to < 50 ps inter-channel delay at the output of the HPOAs. Given a large number of fiber-based components in each of the four low-power channels, their optical path lengths are quite different and the four outputs are not time-aligned as built. Additionally, the four HPOAs have a different amount of gain fiber / passive fiber each, causing further optical path differences. Time alignment is accomplished in two steps, as illustrated in Figure 4. First, the outputs of the four low power channels are time-aligned to each other with a set of optical delay lines (time delay stage 1 in Figure 4), where each channel goes through an individual delay line. Each delay line has a combination of a fixed path-specific delay, and a variable user-adjusted delay. Second, additional set of delay lines (time delay stage 2 in Figure 4) is assigned to the HPOA inputs, so that the inputs to this second set of delay lines are time-aligned to the outputs of the HPOAs. Optical path differences between each HPOA are eliminated by this second set of delay lines, which also include a path-specific fixed delay and a user-adjusted delay.

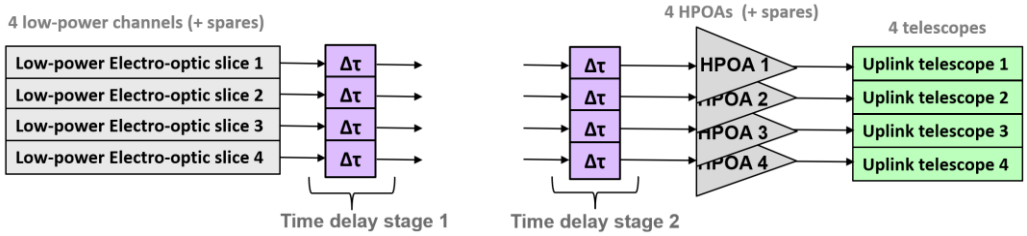

Figure 4. Time alignment / time delay implementation

Having two sets of delay lines provides the flexibility to use any low power channel interchangeably with any HPOA. This would be particularly useful in the unlikely failure of either a low power channel or an HPOA during the mission, requiring spares to be used. Physically, both sets of delay lines are located within a 42U rack, where the second set of delay lines also compensates for the optical path difference in the long single mode fibers used to deliver the signals into and up the gimbaled mount.

Optical amplifiers and uplink telescopes

The system uses commercial-off-the-shelf (COTS) non-polarization maintaining HPOA OEM units with ~40 dB of gain and capable of producing up to 11 W of maximum output power each. All the HPOAs are driven by the same power supply. Each HPOA has an externally spliced 99/1 coupler at the output, where 1% tap is routed back for diagnostics and output signal monitoring, while 99% tap is spliced to an AR-coated fiber connector directly coupled to the uplink telescope. Total length of the fiber between the last gain stage of the HPOA and the end of the AR-coated fiber connector is specified to be under 2.5m, but practically is close to 2m for each HPOA in the system (all fiber is non-PM single mode). The HPOAs and their power supply are mounted on top of the enclosed gimbaled mount directly next to the uplink telescopes.

The uplink telescopes are 15.4 cm refractors custom-built for and reused from the LLCD program [10]. They contain all the optics necessary for fiber-launching collimated 10 W beams into free space, solar windows, optics for adjusting output beam divergence, a fast-steering mirror and back-end optics necessary for tracking downlink signals. The telescopes transmit beacon, filler and comm wavelengths. The four uplink telescopes, two downlink telescopes as well as all the HPOAs and PAT hardware are housed in an enclosed azimuth-over-elevation gimbal. Temperature-controlled forced air circulates through the gimbal to maintain the optics at a particular temperature and to mitigate the heating of the HPOAs.

Telemetry / Diagnostics

System health and other telemetry is constantly monitored, both on the low-power channels and on the HPOA output via a 1% tap. This 1% output of each HPOAs goes through a fiber splitter, as shown in Figure 5. Part of the signal goes to power, optical spectrum, and waveform monitoring; another part of the signal goes into a set of narrowband optical filters centered at uplink comm, beacon and filler wavelengths. Each filter is followed by a power meter. All monitoring channels are calibrated to the actual output of a corresponding HPOA. This allows for automatic monitoring of the output power in acquisition and comm signals separately and to quickly adjust the comm/acquisition ratio as needed. System power is constantly monitored and is quickly adjusted in 3-dB steps as required for the operation. Calibrated wavemeter monitors all system wavelengths and automatic software control loop adjusts source DFB lasers if / when needed. Low power channels allow for power, optical spectrum, and time-domain waveform monitoring at multiple locations within the electro-optic chain.

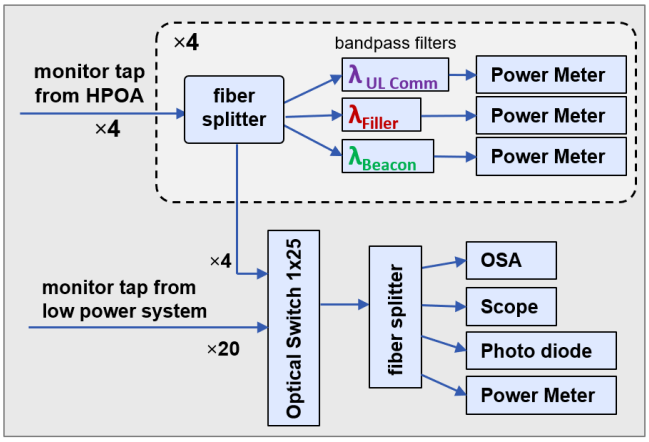

Figure 5. Telemetry / diagnostics path

All uplink transmitter electro-optics up to HPOAs are physically housed in two 42U racks as shown in Figure 6. The racks include all the Comm/Beacon/Filler DFB lasers and their control, all the electro-optics for uplink comm signal and acquisition signal paths shown in Figure 3. FPGA-based data processor with 1x4 RF signal distribution hardware shown in Figure 2, two time-delay stages, electro-optics necessary for output signal monitoring and all the diagnostic equipment listed in Figure 5. It also houses a computer which controls the transmitter and provides live telemetry on the system, which is constantly logged for diagnostic purposes.

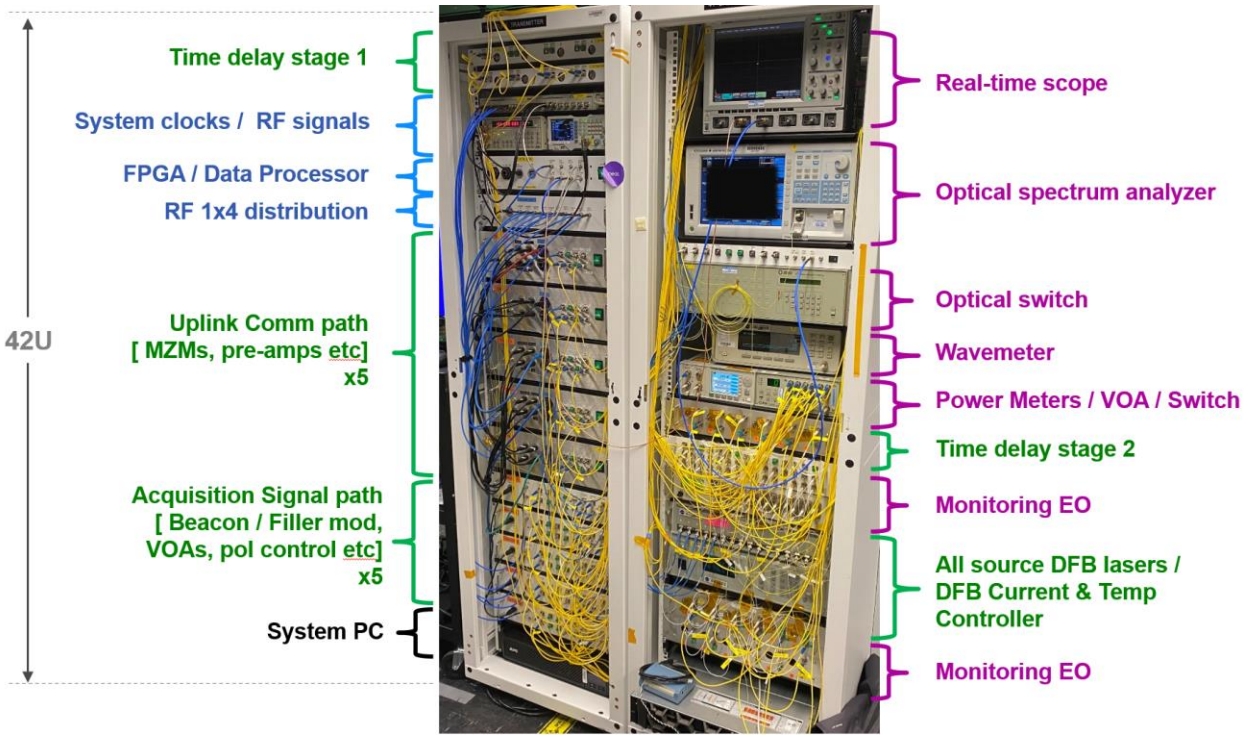

Figure 6. Two 42U racks house all the low power electro-optics and all the diagnostic and monitoring equipment for the transmitter.

3. SYSTEM PERFORMANCE /CHARACTERIZATION

Waveform quality and time alignment

Uplink transmitter waveform was characterized in the time domain by capturing the pulses at both data rates with real time scope and fitting them to the RZ50 profile (Figure 7). Inter-channel time alignment was performed both at the end of time delay stage 1 (low power path), and at the end of the HPOA output fibers shown in Figure 4. For the low power path, each output of the time delay stage 1 was connected to the same photodiode sequentially. The real-time scope was triggered with a separate electrical output from the FPGA data transmitter used for time-of-flight testing, and one of the codeword synchronization marker [11, 14] pulses was captured. Relative inter-channel time delay was estimated from post-processing of the four datasets. Time delay of the high-power path, starting from the input of time delay stage 2 (Figure 4) was measured similarly, but the same low power data source was used as an input to all four high power channels.

For each individual channel, the optical path is the same regardless of the slot rate (250 or 500 MHz). However, the RF signal paths are slot-rate specific: 250MHz RF signals go through physically different set of hardware than 500 MHz signals, before they drive the MZMs. For this reason, we measure the time alignment at each slot rate. The results for low-power path time alignment and the resulting pulse shapes are shown in Figure 7 at both slot rates. The exact inter-channel time delays at both slot rates for low power paths are listed in Table 4.

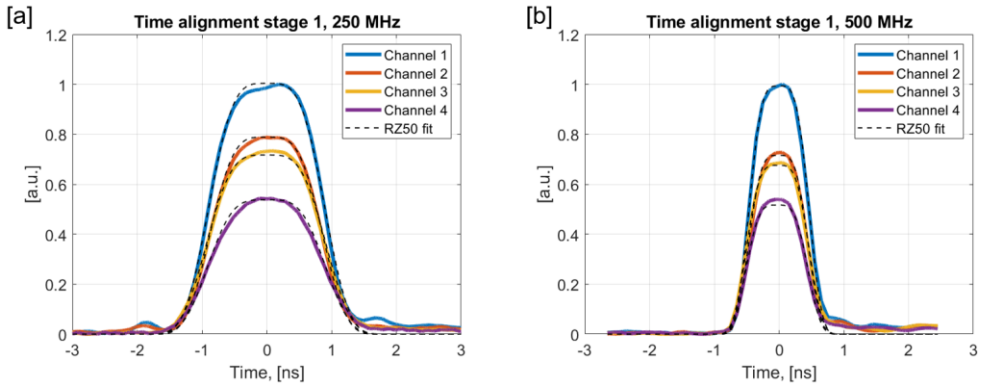

Figure 7. Measured time-domain pulses for each channel, at the output of 1st time delay stage (low power path, prior to the HPOA).

Table 4. Inter-channel delay in low-power path.

	Ch 1	Ch 2	Ch 3	Ch 4
250 MHz	0 ps	8 ps	8 ps	8 ps
500 MHz	0 ps	10 ps	20 ps	32 ps

As evident from Figure 7, the amplitudes of the low power channels are somewhat different. This reflects slightly different per-channel insertion losses and does not affect the actual per-channel output powers since all the HPOAs operate in a saturated regime. The high-power inter-channel delays were separately measured and show similar results with under 15ps per channel delays, confirming the transmitter is in spec with under 50 ps net inter-channel delay.

Extinction ratio (ER) of the uplink comm waveform was measured for each individual channel at two locations – at the output of the low power channels, and at the output of the HPOA while operating at 10 W. The ER was measured for 500 MHz slot rate using a fast real-time scope with a fast photodiode to measure the peak power, pulse duration, and the duty cycle. A separate power meter was used to measure the average power in the signal, and the ER was calculated according to [18] from measured parameters. Table 5 summarizes the results, showing an ER reduction due to the HPOA of 2 to 5 dB depending on the channel.

Table 5. Measured Extinction Ratios at 500 MHz slot rate.

Channel	Low Power (pre-HPOA)	High power (10W)
1	32.2 dB	26.7 dB
2	30.1 dB	26.8 dB
3	26.8 dB	24.7 dB
4	30.0 dB	25.8 dB

Comm / Acquisition ratio control

One of the main system design drivers was the need to rapidly switch the relative amount of acquisition and comm power in the output beam, keeping the combined output power the same. System interface control document [11] tabulates the acquisition-to-comm power ratio values at the output of the HPOAs in steps of 3 dB, to be achieved under 2s, at all specified power levels and keeping beacon and filler powers the same at the HPOA output. This is implemented using three VOAs per channel as shown in Figure 3, and is a combination of a real-time control loop and a look-up table. When the ratio of acquisition / comm power is not being changed by an operator, a real time control loop constantly keeps it within 0.5 dB from its target value while also maintaining the required total output power. When the ratio is changed by an operator, the system first uses VOA values from a look-up table and then fine-adjusts them with the control loop. Ratio switching time was measured to be <1.3 s for all cases of interest. Figure 8 shows uncalibrated optical spectra for three specific cases measured at 10W/channel output power: [a] uplink comm with tracking: the power in the comm beam is

significantly higher than the power in the beacon / filler; [b] transition to fine tracking: the power in beacon and filler are dominating; [c] acquisition: all power is in the acquisition signal.

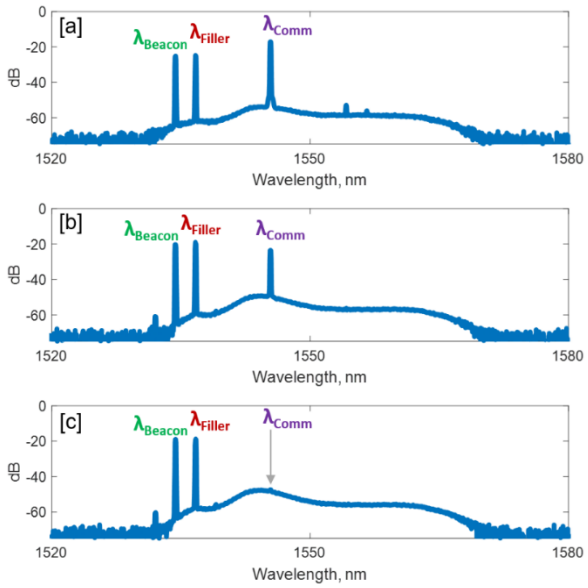

Figure 8. Optical spectra of a subset of acquisition-to-comm ratios as implemented, at 10W output power. [a] Uplink comm with tracking, [b] transition to fine track, [c] acquisition-only

Polarization Control

While each channel is specified to produce up to 10W of average output power, the peak power is 80 times the average power (up to ~800W) due to the shape of RZ50 optical pulses and low duty cycle PPM-32 modulation format with guard slots. Such peak power introduces nonlinear effects such as self-phase modulation and cascaded four-wave mixing (FWM) [12, 13, 18]. Despite the short length (< 2.5m) of each post-HPOA output fiber carrying this high-power optical signal to the uplink telescope input, it is enough to cause system performance degradation due to unmitigated nonlinearities. One effect is the reduction in output power in comm signal as the energy from the main signal is being used to put power into multiple four-wave-mixing side bands. Another, and perhaps more detrimental effect is the blinding of the tracking camera located at the back-end of the uplink telescope assembly with FWM side-bands. Figure 9 shows a high-level schematic of the back-end optics inside of each uplink telescope.

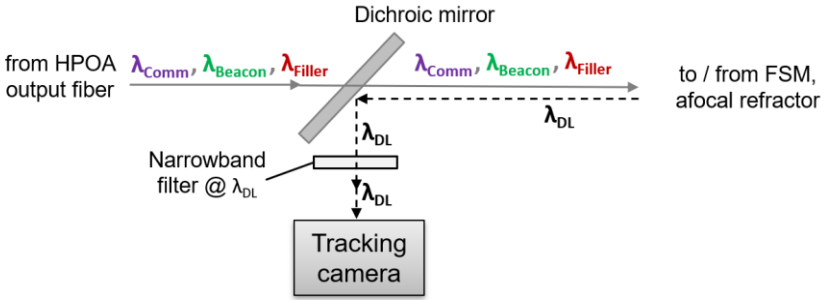

Figure 9. Schematic of the uplink telescope back-end optics. FSM – fast steering mirror, DL – downlink wavelength.

A dichroic filter is located in a collimated space prior to the afocal refractor. It transmits beacon, filler and uplink comm wavelengths, but reflects downlink wavelength coming from the spacecraft towards the tracking camera through a narrow-band optical filter centered around downlink wavelength (λ_{DL} in Figure 9). This signal is used for tracking in conjunction with a fast-steering mirror (FSM). A small portion of the high-power transmit beam scatters from the optics of the afocal refractor back onto the dichroic filter. Everything expect for the downlink signal should be rejected by a subsequent narrowband filter. However, one of the main FWM sidebands is close enough to the downlink wavelength and high enough in power if unmitigated that part of it scatters back into the system, and is transmitted through the narrowband filter blinding the sensitive tracking camera. In practice, this is mitigated by minimizing FWM sidebands by orienting beacon

and filler polarizations orthogonal to that of the uplink comm signal. The remaining polarization controller is used to orient the input to the HPOA in a way that minimizes self-phase-modulation-induced effects and thus lowers the background. Although HPOA is non-polarization maintaining, multiple tests have shown that it has a preferred input polarization state that reduces the SPM effects. Figure 10 shows the output spectrum of a single channel when operating at maximum output power (10W). Figure 10 [a] shows the spectrum with non-optimized polarization and multiple FWM side-bands, including the one within the bandwidth of the narrowband downlink wavelength filter. Figure 10 [b] shows the spectrum of the same channel with polarization optimized to reduce parasitic nonlinear effects. The level of the FWM sideband which overlaps with the downlink wavelength window is minimized to below-the-noise-floor of the tracking camera. This was confirmed by capturing the tracking camera images at full power with optimized and non-optimized polarization levels. In practice polarization control is done via the main control software interface and needs to be adjusted once every few days.

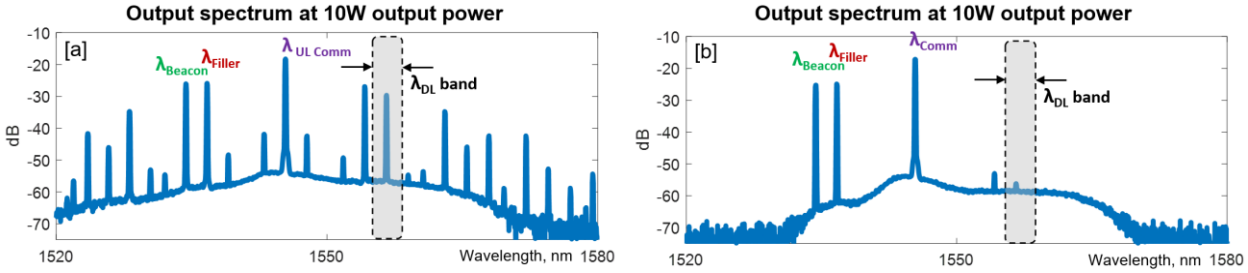

Figure 10. Single channel HPOA output spectrum at 10W. [a] polarization as is; [b] polarization optimized.

Performance against the flight modem receiver

Communications performance of the uplink transmitter in terms of codeword error rate (CWER) is specified at the input to the flight modem pre-amplified receiver, which has been tested and qualified separately. Uplink transmitter was tested against the flight modem receiver in the following manner: each of the four channels were run at 10W maximum power with optimized polarization. The 99% HPOA outputs were terminated into calibrated power meters. The 1% taps were coupled into individual optical delay lines and a subsequent 4x1 fiber combiner, so that at the output of the fiber combiner all 4 channels were aligned to have inter-channel delay under 50 ps. This additional time alignment was done because the 1% tap paths themselves were not part of the main transmit beam and thus are not time-aligned when being monitored. Combined signal passed through an optical filter to remove beacon and filler wavelengths (which during the mission would be routed elsewhere by space terminal's optics), a VOA, and a 3dB splitter.

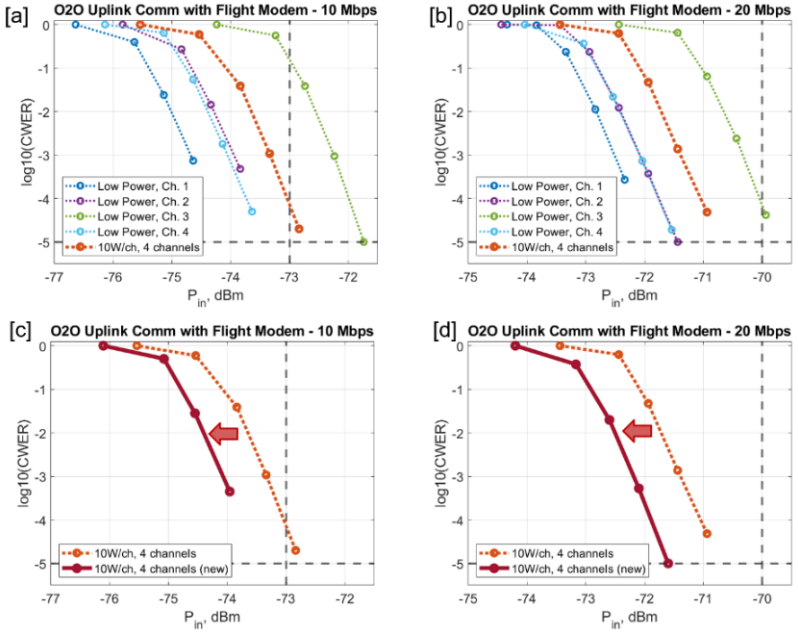

Figure 11. CWER measurements against flight receiver.

One arm of the 3-dB splitter was coupled into a power meter, while the one arm was coupled into the flight modem receiver. CWER was measured while varying the input power into the flight receiver. Separately, each low power channel was tested individually against the flight receiver, to see if the post-HPOA extinction ratio reduction had any effect on the comm performance. The results are shown in Figure 11. During the initial tests, three out of four low power channels were in-family and in-spec at both data rates (Figure 11 [a] and [b]), while the outlier channel (#3) showed a ~2dB penalty with respect to the other three. The high-power 4-channels-combined performance was pulled towards lower sensitivity due to this outlier channel. Subsequent rework of the troubled low-power channel eliminated this problem. The experiments were repeated, and the combined high-power 4-channel system performance improved by ~1dB at both data rates, as shown in Figure 11 [c] and [d]. Dashed grey lines in Figure 11 indicate performance requirements (minimum input power @ $\log_{10}$(CWER)=-5), and the transmitter is shown to be in spec.

Long-duration full-power operations

Long-duration transmitter tests operating at high-power were done on site at NASA's White Sands Complex. Figure 12 shows the temperature of each HPOA (baseplate) as a function of time, when operating all four channels at 2.5W per channel (10W combined output power), and separately when operating at 10W per channel (40W combined output power). When operating at 2.5W output power, the hottest-running HPOA starts converging to a steady temperature near ~35°C, while at 10W/channel output power the hottest running HPOA reaches ~52°C. Longer duration tests (up to 10 hours) were performed, showing stable operation with all HPOAs running at the highest output power. Temperatures higher than 52°C have not been observed, but at longer tests the HPOA temperatures slowly fluctuate reflecting the outside environment (sunrise / sunset / outside temperature changes). The HPOAs may be safely operated up to 60°C.

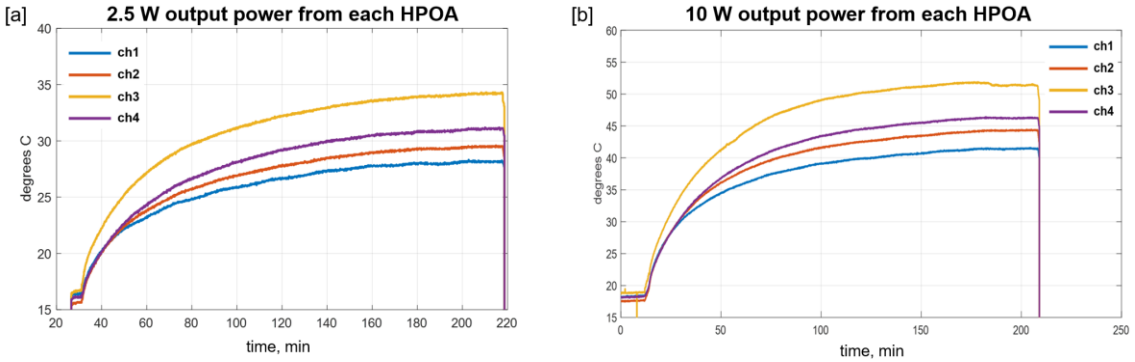

Figure 12. HPOA temperatures during long-term operation, with all 4 HPOAs running at the same time. [a] P(out)=2.5 W/channel, outside temperature 49-59F; [b] P(out)=10W/channel, outside temperature 52-65F;

4. CONCLUSION

The design, implementation, and detailed performance characterization of the O2O uplink transmitter for NASA's Artemis II mission has been presented. The transmitter supports uplink data rates of 10 Mbps and 20 Mbps, implemented with PPM-32 modulation at 250 and 500 MHz slot rates respectively. It consists of four parallel spatial-diversity channels each carrying an acquisition and uplink comm signals which overlap spatially in the far field. The spatial diversity channels are time-aligned to < 50ps, and provide a combined output power of 40W. The transmitter reports real-time telemetry and has automatic real-time wavelength, power and beacon/comm ratio control. It is able to operate self-sufficiently and consistently for multiple hours and shows excellent performance when tested against a flight modem receiver.

The O2O program will enable operational high-data rate optical communications to and from the Orion spacecraft during the proposed Artemis II mission. This will enable real-time video conferencing and high-volume data transfers to and from Orion at lunar distances, opening the door for many capabilities that are not possible with traditional RF-based communication systems.

ACKNOWLEDGEMENTS

The authors acknowledge Scott Henion, Michael Read and David Mathewson from MIT Lincoln Laboratory for help with uplink transmitter implementation; and Stephen Hall, Rich Hovorka and Andrew Wittmeier from Peraton for help with long-duration transmitter measurements.

REFERENCES

[1] S. Creech, J. Guidi and D. Elburn, "Artemis: An Overview of NASA's Activities to Return Humans to the Moon," in *2022 IEEE Aerospace Conference (AERO)*, Big Sky, MT, USA, 2022.

[2] M. Smith, D. Craig, N. Herrmann, E. Mahoney, J. Krezel and N. McIntyre, "The Artemis Program: An Overview of NASA's Activities to Return Humans to the Moon," in *2020 IEEE Aerospace Conference*, Big Sky, MT, USA, 2020.

[3] "https://www.nasa.gov/mission/artemis-i/," NASA. [Online].

[4] B. Robinson, F. Khatri, M. Padula, S. Hotowitz and M. Bay, "Optical Communication for Human Space Exploration--Status of Space Terminal Development for the Artemis II Crewed Mission to the Moon," in *IEEE ICSOS Conference*, 2022.

[5] F. Khatri, M. Bay, J. King, J. Chang, T. Hudson, R. Schulein, O. Mikulina, J. J. Zinchuk, R. McGraw, J. Gregory, P. Gramm, N. Desch, S. Horowitz and B. S. Robinson, "Optical communications operations concept for the Artemis II crewed mission to the Moon," in *Proc. SPIE 12413, Free-Space Laser Communications XXXV*, San Francisco, CA, USA, 2023.

[6] N. Desch, A. Caroglanian, R. George, R. Lafon, T. Rykowski, H. Safavi, C. Finegan, S. Hall, J. Mahaffey and R. Miller, "Ground Segment Operations Concept for the Orion Artemis-2 Optical Communications System," in *16th International Conference on Space Operations*, virtual, 2021.

[7] A. Biswas, S. Piazzolla, A. Croonquist, E. Alerstam, M. Wright, M. Shaw, E. Wallman, R. Rogalin, S. Meenehan, C. Chen and J. Allmaras, "Optical-to-Orion (O2O) ground terminal (GT) at Table Mountain Facility (TMF)," in *Proc. SPIE 12413, Free-Space Laser Communications XXXV*, San Francisco, CA, USA, 2023.

[8] B. Robinson, D. Boroson, D. Burianek, D. Murphy, F. Khatri, J. Burnside and J. Kansky, "The NASA Lunar Laser Communication Demonstration—Successful High-Rate Laser Communications To and From the Moon," in *SpaceOps 2014 Conference*, Pasadena, CA, USA, 2014.

[9] D. Boroson and B. Robinson, The Lunar Laser Communication Demonstration: NASA’s First Step Toward Very High Data Rate Support of Science and Exploration Missions, Springer Cham, 2015, pp. 115-128.

[10] D. Murphy, J. Kansky, M. Grein, R. Schulein, M. Willis and R. Lafon, "LLCD operations using the Lunar Lasercom Ground Terminal," in *Proc. of SPIE Vol. 8971, Free-Space Laser Communication and Atmospheric Propagation XXVI*, San Francisco, CA, USA, 2014.

[11] *Orion ICD Space Terminal Element to Ground Terminal Element (Optical), O2O-ICD-1001*, NASA, MITLL, 2020.

[12] R. Schulein, R. Lafon, M. B. Taylor, P. MacKoul, J. Carney, M. Stevens, B. Robinson, S. Constantine, M. Willis, D. Peckham, B. Zhu, J. Fini and D. Caplan, "Nonlinearity mitigation of a 40-Watt 1.55-micron uplink transmitter for lunar laser communications," in *Proc. SPIE 8610, Free-Space Laser Communication and Atmospheric Propagation XXV*, 2013.

[13] D. O. Caplan, J. Carney, R. Lafon and M. Stevens, "Design of a 40 Watt 1.55μm uplink transmitter for Lunar Laser Communications," in *Proc. SPIE 8246, Free-Space Laser Communication Technologies XXIV*, 2012.

[14] "Optical Communications Coding and Synchronization, CCSDS 142.0-B-1," *The Consultative Committee for Space Data Systems*, 2019.

[15] B. Moison and J. Hamkins, "Coded Modulation for the Deep-Space Optical Channel: Serially Concatenated Pulse-Position Modulation," The Interplanetary Network Progress Report, vol. 42-161, p. 1-25, 2005.

[16] J. Nappier, B. Vyhnalek, S. A. Tedder and N. Lantz, "Characterization of a photon counting test bed for space to ground optical pulse position modulation communications links," in *Proc. SPIE 10910, Free-Space Laser Communications XXXI*, 2019.

[17] F. Miranda, S. Tedder, B. Vyhnalek, J. Downey, A. Wroblewski, C. Bakula, E. J. Karz, J. Lekki, D. R, A. Hylton, D. Raible and R. R. Romanofsky, "An overview of key optical communications technologies under development at the NASA Glenn Research Center," in *Proc. SPIE 11692, Optical Interconnects XXI*, 2021.

[18] D. O. Caplan, "Laser communication transmitter and receiver design," in *J. Opt. Fiber. Commun. Rep.*, Springer Science, 2007.